DOI: 10.1534/genetics.104.038620

A Gene(s) for All-*trans*-Retinoic Acid-Induced Forelimb Defects Mapped and Confirmed to Murine Chromosome 11

Grace S. Lee,* Rita M. Cantor,† Arin Abnoosian,* Euisun Park,* Mitsuko L. Yamamoto,* David N. Hovland, Jr.‡ and Michael D. Collins*,[1]

**Molecular Toxicology Interdepartmental Program, UCLA School of Public Health, Los Angeles, California 90095,* †*Department of Human Genetics and Department of Pediatrics, David Geffen School of Medicine at UCLA, Los Angeles, California 90095 and* ‡*Amgen, Thousand Oaks, California 91320*

Manuscript received November 15, 2004
Accepted for publication February 9, 2005

ABSTRACT

All-*trans*-retinoic acid (RA) induces various anatomical limb dysmorphologies in mice dependent on the time of exposure. During early limb development, RA induces forelimb ectrodactyly (digital absence) with varying susceptibilities for different inbred mouse strains; C57BL/6N are highly susceptible while SWV are resistant. To isolate the genetic basis of this defect, a full-genome scan was performed in 406 backcross fetuses of F_1 males to C57BL/6N females. Fetuses were exposed via a maternal injection of 75 mg of RA per kilogram of body weight on gestational day 9.25. The genome-wide analysis revealed significant linkage to a chromosome 11 locus near D11Mit39 with a maximum LOD score of 9.0 and to a chromosome 4 locus near D4Mit170. An epistatic interaction was detected between loci on chromosome 11 (D11Mit39) and chromosome 18 (D18Mit64). Linkage to the chromosome 11 locus (D11Mit39) was confirmed in RA-treated backcross fetuses of F_1 females to C57BL/6N males. Loci associated with bone density/mass in both human and mouse were previously detected in the same region, suggesting a mechanistic linkage with bone homeostasis. The human syntenic region of this locus has been previously linked to Meckel syndrome; the phenotype includes postaxial polydactyly, an ectopic digital defect hypothesized to be induced by a common molecular pathway with ectrodactyly.

RETINOIDS, vitamin A derivatives, have been effective medications for diseases such as acne, psoriasis, and cancers and are being developed for therapeutic uses in obesity and type II diabetes (Sporn *et al.* 1994; Villarroya *et al.* 2004). However, a major limitation for the use of these compounds remains teratogenicity, as numerous human congenital malformations have been produced by exposure to retinoids during pregnancy (Lammer *et al.* 1985; Dai *et al.* 1992). Retinoids have also been potent teratogens in laboratory animals (Collins and Mao 1999). In most systems in rodents, all-*trans*-retinoic acid (RA) has caused congenital malformations that varied in scope and severity with dose and time of gestational exposure (Shenefelt 1972; Geelen 1979). In this regard, the dose- and time-dependent effects of RA have been studied extensively in developing limbs (reviewed in Lee *et al.* 2004). At early stages of limb bud growth, mouse gestational day (GD) 9.5, 13-*cis*-RA treatment had effects that were primarily restricted to missing digits or ectrodactyly (Sulik and Dehart 1988). Although 13-*cis*-RA induced predominantly right-sided, postaxial ectrodactyly (missing digits on the posterior or ulnar side of the limb), preaxial ectrodactyly (missing digits on the anterior or radial side of the limb) was also induced (Sulik and Dehart 1988). Moreover, inbred strains of mice exhibited differential sensitivity to RA-induced forelimb ectrodactyly, demonstrating the importance of genetic background in sensitivity. When administered at early stages of limb morphogenesis, the C57BL/6N strain showed high sensitivity while the SWV strain showed complete resistance (Collins *et al.* 2005).

The relative strain difference for the induction of preferentially right-sided, postaxial forelimb ectrodactyly was demonstrated for other teratogens, including acetazolamide, cadmium, carbon dioxide, ethanol, and hyperthermia (although the studies used either C57BL/6J or C57BL/6N; reviewed in Lee *et al.* 2004). These agents are the only compounds known where the two strains have been compared for this specific limb defect. This conservation of strain sensitivity to this specific defect induced by multiple teratogens that are presumed to function by different mechanisms suggests that a final common pathway (Wilson 1973) in digital development is more susceptible in the C57BL/6 than in the SWV strain.

Previously, a full-genome scan using backcross fetuses of pooled F_1 (C57BL/6N female × SWV male or its reciprocal cross) males to C57BL/6N females determined chromosomal regions linked with the sensitivity

[1]*Corresponding author:* UCLA School of Public Health, CHS 71-297, 10833 Le Conte Ave., Los Angeles, CA 90095. E-mail: mdc@ucla.edu

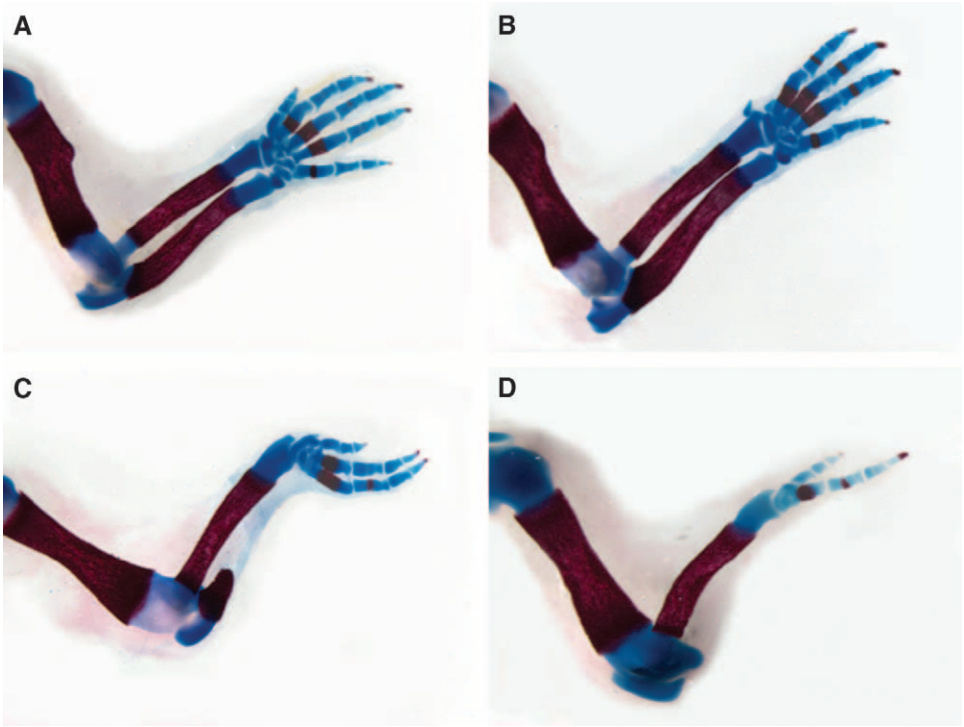

FIGURE 1.—Forelimb defects induced by RA on GD 9.25. (A) Normal paw of right limb, score of 1; (B) right limb ectrodactyly digit 1, score of 3; (C) right limb ectrodactyly digits 4 and 5 and reduction of ulna, score of 6; and (D) right limb ectrodactyly digits 3, 4, and 5 and absence of ulna, score of 9.

to cadmium-induced forelimb ectrodactyly of the same two strains (HOVLAND *et al.* 2000). The analysis identified significant linkage to a locus at the distal end of chromosome 6, with suggestive linkage to loci on chromosomes 11 and 13. In this study, a genome-wide linkage analysis identified loci associated with the same strain difference in RA-induced forelimb ectrodactyly. This analysis used the same backcross design to identify loci contributing to the same differential strain sensitivity of the comparable limb phenotype produced by RA and to compare the identified loci with those that were linked when cadmium was administered.

MATERIALS AND METHODS

Animals and teratology: C57BL/6NCrlBR (C57) mice were obtained from Charles River Laboratories (Hollister, CA). The founder SWV/Fnn (SWV) mice were from Richard Finnell (Texas A&M University). Pooled F_1 (C57 female × SWV male or SWV female × C57 male) males were backcrossed with C57 females to generate BC1 fetuses, and pooled F_1 females were backcrossed with C57 males to generate BC2 fetuses. Mice were kept in a climate-controlled room under an alternating 12-hr light/dark cycle. Timed matings were produced by placing a male into cages with multiple females for the last 2 hr of the dark cycle. The time of vaginal plug detection was designated the start of GD 0. On GD 9.25, RA (Sigma, St. Louis) was dissolved in 100% ethanol (8% of the dosing solution volume), suspended in soybean oil (92% of the dosing solution volume), and administered to pregnant mice by intraperitoneal injection at a dose of 75 mg/kg body weight. All steps involving RA were performed under dim yellow light to prevent photoisomerization. On GD 18, maternal mice were killed, and the numbers of implantation and resorption sites, viable fetuses, and gross malformations were recorded. Each fetus was stained with alizarin red and alcian blue for skeletal analysis as described previously (HOVLAND *et al.* 2000). The litter was considered the statistical unit for comparisons of resorption and malformation rates due to the significant litter effect and subsequent lack of independence of fetal data. Differences between crosses in average litter percentages were assessed by *t*-test for significance ($P < 0.05$). Tests for fetal incidence of forelimb defects in Table 2 were performed using the 2×2 χ^2 test of fetal forelimb defects. Statistical significance was inferred at a *P*-value of 0.05.

A method for determining the relative developmental timing of the various murine crosses was deemed valuable. Embryos from the parental strains and the two backcrosses, BC1 and BC2, were collected on GD 9.25, and the somites, which are dorsal segmental mesodermal condensations that develop one at a time in a craniocaudal direction during early organogenesis, were counted as a gross indicator of the embryonic developmental stage at the time of treatment. The median somite number of the embryos was the indicator of the developmental stage of a litter, and a mean for multiple litters (medians) was calculated.

Phenotyping: Each fetus was phenotyped for forelimb malformations as a binary trait and scored for the severity of the defect as a semiquantitative trait. Forelimb defects were also classified by axiality (preaxial or postaxial) and laterality (left or right). The severity of a forelimb malformation was scored according to a previously described system (HOVLAND *et al.* 2000; see Figure 1). The system arbitrarily assigned a normal pair of forelimbs a score of 1. For each shortened or rudimentary digit or visually significant thinning of a digit, one point was added to the fetal forelimb score. The total absence of a single digit added two points to the score, and each additional missing digit added two more points. A visually significant reduction in the length of the humerus, radius, or ulna was given a single point, and the complete absence of any of these long bones was accorded two points. Fusion of the ulna and the radius added a point. Thus, scores ranged from 1, for a fetus with two normal limbs, to 33, for a fetus with bilateral amelia. To minimize the influence of outliers, a natural log transformation was applied to the semiquantitative trait prior to the QTL analysis.

Genotyping: Fetal visceral genomic DNA was isolated by

TABLE 1

Reproductive and selected-malformation percentages for backcross fetuses treated on GD 9.25 with 75 mg of RA per kilogram of body weight

Cross	Total no. of litters	Total no. of implants/collected fetuses[a]	Mean litter % of resorptions[b]	Mean litter % forelimb defects[b]	Mean litter % hindlimb defects[b]	Mean litter % cleft palate[b]
C57♀ × F_1♂	101	831/419[c]	49.7 (±3.5)	28.2 (±3.1)[d]	3.2 (±1.8)	27.5 (±3.3)[d]
F_1♀ × C57♂	91	1020/569[e]	44.0 (±3.8)	38.5 (±3.7)[d]	0.6 (±0.4)	37.6 (±2.8)[d]

[a] Collected fetuses included dead fetuses.
[b] Parenthetical value represents the standard error of the mean.
[c] Thirteen of 419 fetuses were not genotyped due to the poor quality of isolated DNA.
[d] Mean percentage significantly different between crosses, *t*-test, $P < 0.05$.
[e] Twenty-four of 569 fetuses were not genotyped due to the poor quality of isolated DNA.

phenol/chloroform extraction. From 419 collected BC1 fetuses, 13 fetuses were not genotyped due to poor quality of isolated DNA. Similarly, 24 of 569 collected BC2 fetuses were not genotyped. Some of these fetuses that were not genotyped had forelimb defects. Thus, the numbers of affected and nonaffected fetuses that were used for QTL analyses were slightly different from the numbers of fetuses that were analyzed for teratology results in Tables 1 and 2. Initially, 406 fetuses from BC1 were genotyped by the Center for Inherited Disease Research (CIDR; Johns Hopkins University, Baltimore). Microsatellite markers were screened for polymorphisms between C57 and SWV, and 86 markers spanned the entire genome excluding the Y chromosome. The genotyping was performed by the CIDR PCR protocol (http://www.cidr.jhmi.edu/mouse/protocol.html). The missing data rate was 4.7%, and quality control included 20 blind duplicates. The average spacing between markers was 15.4 cM, with no gaps >34 cM. Subsequently, 3 additional markers on chromosome 11, 1 marker on chromosome 4, and 1 marker on chromosome 6 were genotyped using PCR with 5′-end-labeled forward primers according to procedures from a previous study (Hovland *et al.* 2000). The additional marker on chromosome 6 that was subsequently genotyped was a marker close to the QTL peak for cadmium-induced forelimb defects in the Hovland *et al.* (2000) study. Replication of BC1 loci was done with 545 BC2 fetuses that were genotyped for 3 markers on chromosome 4 and 9 markers on chromosome 11. The missing data rate for the nonautomated genotyping was 1.9%.

Linkage analyses and epistatic interactions: The linkage map was constructed using the MAPMAKER/EXP V3.0b (Lander *et al.* 1987) and Map Manager QTXb19 (Manly *et al.* 2001) software packages using the Kosambi map function. For autosomal linkage, single-marker analysis, interval mapping, and composite interval mapping were performed using the QTL Cartographer V2.0 (Wang *et al.* 2005) software package. To assess whether different anatomical forelimb defects were linked to the same loci, each binary trait was analyzed separately. That is, linkage analysis for the preaxial defect was performed on the progeny with only preaxial and pre- and postaxial defects classified as "affected" and all others as "unaffected." Furthermore, the permutation features of Map Manager QTX and QTL Cartographer were used to establish the genome-wide thresholds for suggestive ($\alpha = 0.63$), significant ($\alpha = 0.05$), and highly significant ($\alpha = 0.001$) linkage with 10,000 and 1000 iterations, respectively. The BC2 fetuses were evaluated for linkage with the entire chromosome 11 and a specific region of chromosome 4. Since the number of markers examined in the BC2 verification was relatively small when compared with the whole-genome scan, the issue of multiple comparisons was reduced, permitting a higher *P*-value for significance. For this purpose, the *P*-value <0.01 was suggested by Lander and Kruglyak (1995). Although the genome-wide *P*-value of 0.05 was designated as significant, this equates to a *P*-value of <0.001 at each individual marker; hence the *P*-value of <0.01 represents a reduction in stringency. Significant threshold levels from the BC1 fetuses were also used for linkage analyses in BC2 fetuses. Searches for pairwise epistatic interactions between loci were performed using Map Manager QTX and verified using the SAS V8 software (SAS Institute, Cary, NC) for a logistic regression procedure and two-way analyses of variance (ANOVA).

RESULTS

Phenotypes of RA-induced forelimb malformations: Relevant reproductive and developmental parameters in the two backcrosses have been summarized in Tables 1 and 2, with specific details regarding the limb malfor-

TABLE 2

Forelimb defect percentages for backcross fetuses treated on GD 9.25 with 75 mg of RA per kilogram of body weight

	Axiality of paw defects (no. of fetuses)			Laterality of limb defects (no. of fetuses)		
				Unilateral		
Cross	Preaxial	Postaxial	Pre- and postaxial	Right	Left	Bilateral
C57♀ × F_1♂[a]	27.7% (26)[b]	40.4% (38)[b]	30.9% (29)	62.8% (59)	5.3% (5)	31.9% (30)
F_1♀ × C57♂	67.7% (130)[b]	11.5% (22)[b]	20.8% (40)	52.6% (101)	8.9% (17)	38.5% (74)

[a] One fetus was not included in axiality of paw defects because this fetus had absence of digit 3.
[b] Significantly different between crosses, 2 × 2 χ^2 test, $P < 0.05$.

TABLE 3

Embryo somite numbers at GD 9.25

Cross	No. of counted embryos (no. of litters)	Mean litter median of somite no. (±SEM)	Somite range
C57♀ × C57♂	133 (16)	21.9 ± 0.3	3–26
SWV♀ × SWV♂	217 (19)	19.3 ± 0.4[a]	5–23
C57♀ × F_1♂	203 (26)	21.3 ± 0.2	9–26
F_1♀ × C57♂	370 (35)	21.7 ± 0.3	3–26

[a] Significantly different from other values using two-tailed *t*-test, $P < 0.05$.

mations. All fetuses exhibited anal atresia and tail agenesis, which indicated fetal exposure to RA (Collins *et al.* 2005). Forelimb defects and cleft palate were the predominant gross malformations observed among the backcross fetuses aside from anal and tail agenesis, consistent with a previous study (Collins *et al.* 2005). Forelimb defects were noted in 28% (mean litter percentage) of BC1 fetuses and 39% of BC2 fetuses (Table 1). Forelimb defects were either unilateral or bilateral; and among the unilateral, right-sided defects were more common than left sided (92% *vs.* 8% in BC1 fetuses and 86% *vs.* 14% in BC2 fetuses; Table 2). Moreover, when the forelimb defects were bilateral, they were more severe on the right than on the left side (60% *vs.* 17% in BC1 fetuses and 58% *vs.* 20% in BC2 fetuses, with the remainder being bilaterally equivalent). In affected BC1 fetuses, there were approximately equal numbers of preaxial and postaxial defects, whereas in affected BC2 fetuses, preaxial defects predominated. In both groups of backcross fetuses, hindlimb defects were rarely observed (Table 1). Additionally, whenever a cross involved F_1 mice, the direction of the breeding to produce the F_1 (either C57 × SWV or SWV × C57) did not produce a significant difference in the incidence of forelimb defects (data not shown). More specifically, incidences of preaxial and postaxial defects were also not significantly different when the maternal animal was either C57 or SWV for the F_1 mice (data not shown).

To assess whether the differences in teratogenic outcome in reciprocal crosses could be explained by developmental staging, the somite values were compared. As shown in Table 3, the somite number of C57 embryos was greater than that of SWV, indicating that C57 embryos were more developmentally advanced than SWV. Moreover, the somite numbers of embryos from the BC1 and BC2 were not significantly different from embryos of the C57 strain, indicating approximate developmental timing equivalence at the time of RA administration for both crosses.

Whole-genome scan: To identify loci containing genes that contribute to the differential sensitivity of C57 and SWV mice to RA-induced forelimb defects, a whole-genome scan was performed in BC1 fetuses on traits listed in Table 4. Results from the full-genome scans, based on the 88 markers, revealed highly significant linkage to a chromosome 11 locus and significant linkage to a chromosome 4 locus (Figure 2). The trait in all affected fetuses (All-1) was significantly linked to a chromosome 11 region near D11Mit39, with a maximum LOD score of 9.0 (Table 4; Figure 3A). Analyses of subsets of this binary trait (Pre-1, Post-1, Left-1, and Right-1) in the same sample population revealed significant linkage to the same location on chromosome 11, but with lower LOD scores, presumably due to the reduced number of affected fetuses (Table 4; Figure 3A). The semiquantitative trait, QT-1, was also significantly linked to the same locus on chromosome 11. Accordingly, this locus was named *Rafar* (*RA*-induced *f*orelimb *a*utopod *r*eduction defect). In addition, the analysis for QT-1 showed significant linkage to a locus on chromosome 4 at D4Mit170 with a LOD score of 2.7 (which exceeded the experiment-wise threshold). This locus was also detected in the binary trait analyses at the suggestive level of significance.

Interaction: Interactions between loci associated with RA-induced forelimb defects were identified using Map

TABLE 4

Linked loci from interval mapping on chromosome 11 for RA-induced forelimb defects in BC1 fetuses

Trait	Abbreviation	No. of affected/ no. of unaffected	Peak position (cM) [a,b]	Marker nearest peak	LOD score [b]
All affected	All-1	93/313	46.3	D11Mit39	9.0
Preaxial	Pre-1	55/351	43.7	D11Mit39	4.5
Postaxial	Post-1	66/340	46.3	D11Mit39	4.8
Right-sided	Right-1	89/317	49.0	D11Mit39	8.6
Left-sided	Left-1	34/372	41.0	D11Mit4	3.2
ln QT [c]	QT-1	93/313	45.0	D11Mit39	6.2

[a] Positions were interpolated to distances described in the MGI (http://www.informatics.jax.org).

[b] Results were from QTL Cartographer, and identical results were also obtained by MAPMAKER/QTL V1.1b and Map Manager QTXb19.

[c] Natural log transformed semiquantitative trait.

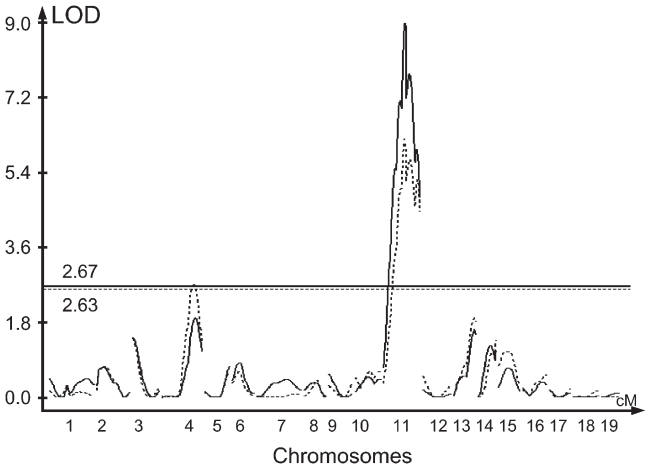

FIGURE 2.—Whole-genome scan of RA-induced forelimb defects in BC1 fetuses generated by QTL Cartographer. The solid curve and solid horizontal line show the LOD score and the 95% LOD score significance threshold, respectively, for the All-1 trait, whereas the dashed curve and the dashed horizontal line show the LOD score and the 95% LOD score significance threshold for the QT-1 trait. The thresholds established by Map Manager QTX and QTL Cartographer were similar.

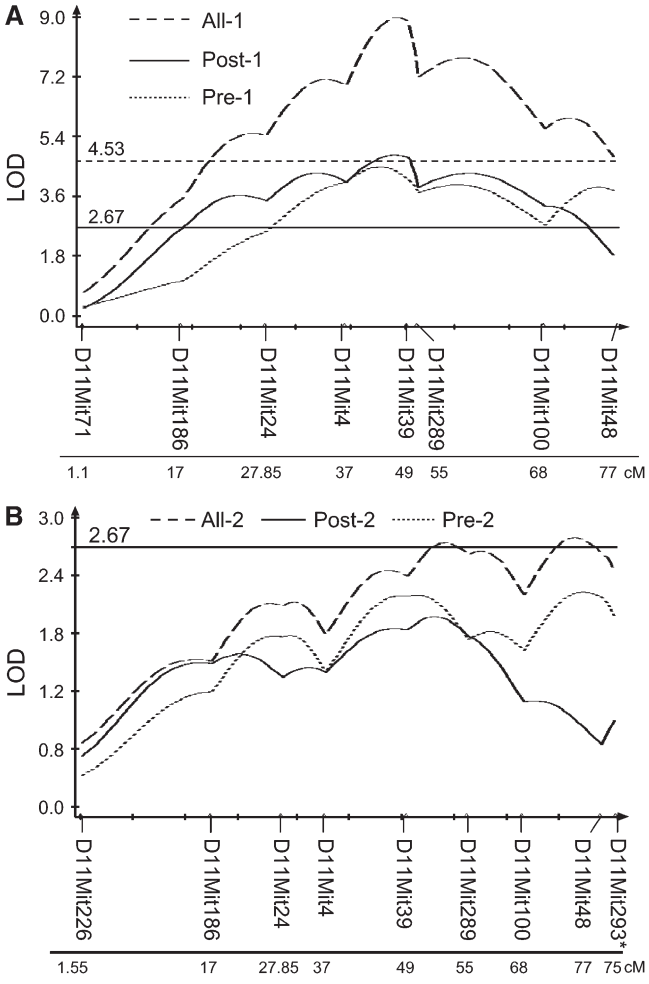

FIGURE 3.—Chromosome 11 linkage maps of RA-induced forelimb defects generated by QTL Cartographer (A) in BC1 fetuses and (B) in BC2 fetuses. The marker positions correspond to linkage distances found in the Mouse Genome Informatics Database (MGI; http://www.informatics.jax.org). The solid horizontal line shows the 95% LOD score significance threshold, whereas the dashed horizontal line shows the 99.9% LOD score significance threshold. According to the linkage map distance in MGI, D11Mit293 is located at 75 cM, but this marker is located more distally than D11Mit48 according to the physical map distance.

Manager QTX, which reported the positions of interacting loci, the joint LOD score of the interaction, and a LOD score for the epistatic effect. As shown in Table 5, when the All-1 trait was analyzed, there was an epistatic component with a LOD score of 2.4 for *Rafar* and a locus on chromosome 18 (D18Mit64). Two-way ANOVA and logistic regression analyses also revealed an epistatic interaction between the chromosomes 11 and 18 loci (Table 5). However, no epistatic interaction was observed between the loci on chromosomes 11 and 4 by two-way ANOVA or logistic regression analysis.

The genotypes of fetuses at three loci, D11Mit39, D18Mit64, and D4Mit170, were examined for interactions by stratifying to assess whether the contribution to the forelimb defect at one locus was independent of the genotype at another locus (Table 6). Taken individually, homozygous (CC) and heterozygous (CS) fetuses at the chromosome 11 locus had 35 and 9% limb malformations, respectively, whereas at the chromosome 18 locus the CC and CS fetuses had 24 and 21%, respectively, and at the chromosome 4 locus the CC and CS fetuses had 29 and 31%, respectively. When fetuses were stratified by their genotypes at the most significantly linked locus, D11Mit39, 43% of fetuses homozygous at both D11Mit39 and D18Mit64 had forelimb defects, while 28% of fetuses that were CC at D11Mit39 and CS at D18Mit64 were affected. The relative order of the intensity of the phenotypic effect induced by the chromosome 18 locus was reversed for fetuses that were CS at D11Mit39, with 4% of D18Mit64 CC fetuses affected and 13% of CS affected. This indicated that the genotype at the chromosome 11 locus altered the effect of the putative risk gene on chromosome 18. The same pattern was observed when the data were analyzed as a quantitative trait (QT), taking the severity of the defects into account instead of the percentage of affected fetuses (Table 6). However, when analogous comparisons were performed for D4Mit170, the effects of the chromosome 11 locus were not comparable (Table 6).

Verification of chromosome 11 linkage in backcross fetuses of F_1 females to C57 males: To assess whether the observed QTL on chromosome 11 could be replicated, linkage analysis was performed in BC2 fetuses for nine markers on chromosome 11. The analysis of the all affected binary trait (All-2) and semiquantitative trait (QT-2) using the 545 fetuses of this alternative cross revealed significant ($\alpha = 0.05$) linkage to a location near

TABLE 5

Loci interaction in RA-induced forelimb defects in BC1 fetuses

Locus 1	Locus 2	Trait	Joint LOD [a]	Locus 1 LOD [a, b]	Locus 2 LOD [a, b]	Epistasis LOD [a]	Locus 1 *P*-value [c]	Locus 2 *P*-value [c]	Interaction *P*-value [c]
Chr11 D11Mit39	Chr18 D18Mit64	All-1	9.8	7.3	0.1	2.4	<0.0001	NS	0.006
		Pre-1	5.7	3.9	0.0	1.7	<0.0001	NS	0.03
		Post-1	6.7	4.9	0.1	1.8	<0.0001	NS	0.01
		Right-1	10.4	8.0	0.1	2.4	<0.0001	NS	0.003
		QT-1	6.7	4.9	0.0	1.7	<0.0001	NS	0.009

[a] Results are from Map Manager QTX using interaction, χ^2 test, $P = 1.0 \times 10^{-5}$.
[b] Locus 1 and locus 2 LOD scores were calculated by single-marker analysis using additive regression model.
[c] Results were generated by SAS program. For binary traits, logistic regression was used; for semiquantitative trait, two-way ANOVA was used. NS, nonsignificant.

D11Mit39 with LOD scores of 2.7 and 3.0, respectively (Figure 3B for All-2; data not shown for QT-2). Thus, the *Rafar* locus was confirmed (Lander and Kruglyak 1995). In addition to *Rafar*, a separate peak was detected at the distal end of chromosome 11 (D11Mit48) in BC2 fetuses (for All-2, a LOD score of 2.8). In the BC2 offspring, the malformation was predominantly preaxial, in contrast to the BC1 cross. The second locus on chromosome 11 (D11Mit48) remained after conditioning on D11Mit39 and using composite interval mapping on the population that included preaxial defects (All-2 and Pre-2), but not on populations that included exclusively postaxial defects (Post-2, data not shown). When using the same procedure but conditioning on D11Mit48, the *Rafar* locus was significant, implying the presence of two separate loci. In the BC1 cross, the D11Mit48 locus was identified in the preaxial population (Pre-1), but not in the other populations (Post-1 and All-1). Thus, the peak near D11Mit48 was associated with the preaxial forelimb defect and not with the postaxial defect. Alternatively, the D11Mit39 peak was associated with both the preaxial and the postaxial defects. In addition, three markers on chromosome 4 in the region of the previously identified significant locus (D4Mit170) were genotyped in BC2 fetuses; however, unlike chromosome 11, no suggestive or significant linkage was detected.

DISCUSSION

This study describes the use of a genetic approach to explain a mouse strain difference in a teratogenic response to RA. Although the somite numbers for the two parental strains were found to be significantly different at the time of RA administration in this study (Table 3), previous experiments have produced evidence to suggest that the difference in teratogenic response is not due to this factor (Collins *et al.* 2005). The described whole-genome scan using a backcross design (C57 female × F_1 male) identified loci on chromosome 11 near D11Mit39 (*Rafar*) and chromosome 4 near D4Mit170 that had significant linkage between the C57 genotype and forelimb ectrodactyly. An independent sample of fetuses from the reciprocal cross (F_1 female × C57 male) provided replication of the linkage to the *Rafar* locus. Further, a second locus on chromosome 11 near D11Mit48 was linked to preaxial ectrodactyly. Although preaxial and postaxial phenotypes are anatomically distinct, the *Rafar* locus was associated with both pheno-

TABLE 6

Stratification by genotype to assess interactions with D11Mit39

Locus 1	Locus 2	Locus 1 genotype	Locus 2 genotype	No. of progeny	No. of affected progeny	% with forelimb defect	Mean QT (±SEM)
D11Mit39	D18Mit64	CC	CC	84	36	42.9	2.9 (±0.4)
		CC	CS	106	30	28.3	2.1 (±0.2)
		CS	CC	81	3	3.7	1.3 (±0.2)
		CS	CS	109	14	12.8	1.7 (±0.2)
D11Mit39	D4Mit170	CC	CC	90	38	42.2	3.1 (±0.4)
		CC	CS	105	29	17.6	2.1 (±0.3)
		CS	CC	77	11	14.3	2.1 (±0.3)
		CS	CS	113	8	7.1	1.3 (±0.2)

C, allele for C57; S, allele for SWV.

types (Table 4). A previous genome scan performed to examine the same strain difference for the same malformation after cadmium administration (Hovland *et al.* 2000) identified a linked locus on chromosome 11; however, the loci are separated by 20 cM (D11Mit39 *vs.* D11Mit24), leading to the supposition that they are distinct.

QTL replication is a useful tool for assessing the value of a linkage result in the presence of the stochastic fluctuation of teratogenic induction. The QTL on chromosome 4 was not replicated in BC2 fetuses, which might be due to the relatively small percentage of the variance (2.7%) explained by this locus making it difficult to repeat or due to a type I statistical error in the first sample. Significantly, *Rafar* was replicated in BC2 fetuses. However, in neither cross was the *Rafar* peak confined to a narrow chromosomal region. Precision of QTL location is limited by the number of recombinants in the chromosomal region (Darvasi 1998). Alternatively, the broad peak may have been due to multiple loci on chromosome 11 that contributed to the strain difference in expression of the phenotype, as demonstrated in several QTL studies (reviewed in Moore and Nagle 2000). For instance, a genome-wide QTL analysis for type I diabetes initially identified a broad peak on murine chromosome 3, designated *Idd3* (Todd *et al.* 1991), but subsequent congenic strain analyses showed that linkage was due to at least four separate loci, *Idd3*, *Idd10*, *Idd17*, and *Idd18* (Podolin *et al.* 1997, 1998). Although there are instances of multiple genes for a single trait mapping to a broad chromosome region like the one seen here, it is equally likely that the delineated broad QTL peak is due to the impact of a single gene.

Generally, interval mapping for fully quantitative traits is more powerful than the mapping methods for binary traits (Xu and Atchley 1996). However, in this study, binary trait analysis resulted in a higher LOD score than linkage analysis of the semiquantitative trait. The numerical system for scoring the malformation was arbitrary and may not have reflected the defect severity as accurately as a binary model.

Although the analyses detected chromosomal loci with statistically significant linkage to the strain difference, the percentage of the variance described by these loci was modest. The percentage of variance explained by *Rafar* was 7.5% and by the chromosome 4 locus was 2.7% for QT-1 (data not shown). Linkage to other loci may be masked by interactions. A chromosome 18 locus was found to interact with the *Rafar* locus, so that even though the chromosome 18 locus LOD score individually was not significant in the full-genome scan, the combined effect of the chromosome 18 and *Rafar* loci had a LOD score that was greater than the sum of the two LOD scores (Table 5). In fact, the contribution of the chromosome 18 locus was dependent on having a specific genotype at the *Rafar* locus (Table 6). It is

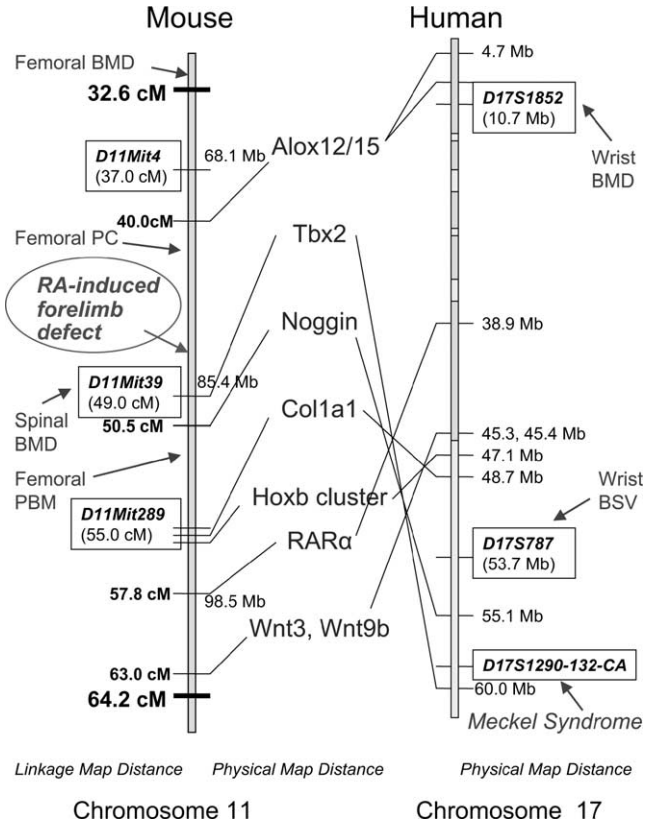

Figure 4.—The two-LOD confidence interval of the *Rafar* locus, its syntenic region in humans, and candidate genes in this region. Linkage map distances in mice were derived from MGI (http://www.informatics.jax.org), and physical map distances were derived from Ensembl Mouse and Human Genome Database (http://www.ensembl.org). Identified QTL for osteoporosis measuring bone mineral density (BMD), peak bone mass (PBM), periosteal circumference (PC), or bone size variation (BSV) and for Meckel syndrome are included.

hypothesized that such interactions may substantially increase the proportion of genetic explanation of the variation between strains. However, the data summarized in Table 6 are not consistent with the classic definitions of negative epistasis, as introduced by Bateson (1909), but are consistent with a lack of additivity, as introduced by Fisher (1918). In a recent analysis of this poorly defined term, Cordell (2002) indicates that epistasis can sometimes be identified statistically, but not understood mechanistically. Our data fall into the latter category and await replication to indicate whether this observation is a type I statistical error or something to be investigated further.

Interestingly, the human syntenic region to *Rafar* has been associated with Meckel syndrome (OMIM 249000; Paavola *et al.* 1995). Meckel syndrome is characterized by cystic kidneys, occipital encephalocele, fibrotic changes of the liver, and postaxial polydactyly, and patients with this syndrome die within a few days after birth (Jones 1997). Relatively short bowed limbs, syndactyly, simian crease, clinodactyly, and preaxial polydactyly are occa-

sionally observed in Meckel syndrome patients (Majewski *et al.* 1983; Jones 1997). The syndrome was originally mapped to human 17q21–24 in a Finnish population (Paavola *et al.* 1995) and was later narrowed to <1 cM on 17q23 (Paavola *et al.* 1999). The mouse region homologous to the human Meckel syndrome region was identified as a 1-cM interval from 49 to 50 cM on murine chromosome 11 (Hentges *et al.* 2004). This is in the same location as *Rafar* (Figure 4). The apparent discordance of polydactyly in Meckel syndrome patients *vs.* ectrodactyly in RA-exposed mice may result from a common molecular developmental mechanism. The mechanism was delineated by a progressive reduction in the dose of Hox gene products, which caused polydactyly at low levels of deficiency and then ectrodactyly and finally adactyly as the deficiency increased (Zákány *et al.* 1997).

Several studies have mapped murine bone mass or density to chromosome 11 regions comparable to *Rafar* (Figure 4). Femoral peak bone mass was linked to chromosome 11 region 51.8 cM between D11Mit90 and D11Mit59 in the SAMP6 spontaneous osteoporotic murine strain (Shimizu *et al.* 1999), a strain with impaired osteoblastogenesis (Jilka *et al.* 1996). The chromosome 11 region between 31 and 49 cM was associated with femoral peak bone mineral density (Beamer *et al.* 2001), spinal peak bone mineral density (Benes *et al.* 2000), and periosteal circumference of the femur (Masinde *et al.* 2003). Wrist bone mineral density and bone size variation in the human was associated with a region on chromosome 17 syntenic with the *Rafar* region (Deng *et al.* 2002, 2003). Thus, multiple studies have indicated an association between bone homeostatic mechanisms and positions on chromosome 11 consistent with the location of *Rafar*, and C57BL/6J mice have been shown to exhibit low bone density in comparison with other strains (Beamer *et al.* 1996).

Multiple candidate genes that are involved in limb development, including lipoxygenase 12/15 (Alox12/15), Tbx2, Noggin, procollagen type 1 alpha 1 (Col1A1), Hoxb cluster, RARα, Wnt3, and Wnt9b (also known as Wnt14b or Wnt15) are within a two-LOD confidence interval of the *Rafar* (32.6–64.2 cM; Figure 4). RARα is one of three subtypes of the nuclear receptors for RA. A previous study has shown that an RARα agonist caused ectrodactyly in mice, while RARβ or RARγ agonists did not (Elmazar *et al.* 1996). Further, Wnt signaling may be a good candidate pathway for RA-induced forelimb defects (as well as osteoporosis). Wnt3 conditional mutant mice and the Wnt coreceptor lipoprotein receptor-related protein (Lrp) 6 mutant mice exhibited distal truncations of the limbs similar to RA-induced forelimb ectrodactyly in this study (Pinson *et al.* 2000; Barrow *et al.* 2003). In addition, *Wnt7a* mutant mice also lack posterior digits (Parr and McMahon 1995), and although this gene is not in the chromosome 11 region it has been shown that Wnt5a and Wnt5b coordinately regulate chondrogenesis (Yang *et al.* 2003), suggesting the possibility that a Wnt in the chromosome 11 region could function with a Wnt that is not. Moreover, Lrp5, another Wnt coreceptor, has been shown to regulate bone density (Kato *et al.* 2002), and inactivating mutations in the human gene result in osteoporosis-pseudoglioma syndrome (Gong *et al.* 2001). Aspects of chondrogenesis, which precede endochondral ossification in the limb, are dependent on Wnt signaling (Daumer *et al.* 2004). Collectively, these data suggest that the Wnt signaling pathway may play an important role in forelimb reduction defects by alteration of limb patterning or limb skeletogenesis.

This study has detected and verified a locus on mouse chromosome 11, *Rafar*, that is associated with the difference between C57 and SWV strain susceptibility to RA-induced preaxial and postaxial forelimb ectrodactyly. A second locus on the same chromosome was associated with preaxial ectrodactyly. Future studies will focus on determining the number of loci on chromosome 11 and their relative contribution to the trait by the creation of congenic mice that parse the chromosome 11 regions of interest. There may be an association between bone density/mass and susceptibility to this malformation. Candidate genes for describing the strain difference in susceptibility include RARα and Wnt3/9b, and interactions between the Wnt and retinoid pathways have not been well delineated. Furthermore, the human Meckel syndrome gene is a candidate for the murine phenotypic difference. Delineation of the mechanisms involved in this teratogenic gene-environment interaction will facilitate an understanding of how multiple factors contribute to the induction of a congenital malformation.

We thank Diana Shih and Heather Cordell for comments and suggestions and Naoko Kono for statistical assistance. We also thank Shengchu Wang for modification of the QTL Cartographer software. This work was supported by the National Institutes of Environmental Health Sciences, R01-ES-010413, and the University of California Toxic Substances Research and Teaching Program's Lead Campus Program in Toxic Mechanisms. Genotyping services were provided by the Center for Inherited Disease Research (CIDR). CIDR is fully funded through a federal contract from the National Institutes of Health to Johns Hopkins University, contract no. N01-HG-65403.

LITERATURE CITED

Barrow, J. R., K. R. Thomas, O. Boussadia-Zahui, R. Moore, R. Kemler *et al.*, 2003 Ectodermal Wnt3/beta-catenin signaling is required for the establishment and maintenance of the apical ectodermal ridge. Genes Dev. **17:** 394–409.

Bateson, W., 1909 *Mendel's Principles of Heredity.* Cambridge University Press, Cambridge, UK.

Beamer, W. G., L. R. Donahue, C. J. Rosen and D. J. Baylink, 1996 Genetic variability in adult bone density among inbred strains of mice. Bone **18:** 397–403.

Beamer, W. G., K. L. Shultz, L. R. Donahue, G. A. Churchill, S. Sen *et al.*, 2001 Quantitative trait loci for femoral and lumbar vertebral bone mineral density in C57BL/6J and C3H/HeJ inbred strains of mice. J. Bone Miner. Res. **16:** 1195–1206.

Benes, H., R. S. Weinstein, W. Zheng, J. J. Thaden, R. L. Jilka *et al.*, 2000 Chromosomal mapping of osteopenia-associated quan-

titative trait loci using closely related mouse strains. J. Bone Miner. Res. **15:** 626–633.

Collins, M. D., and G. E. Mao, 1999 Teratology of retinoids. Annu. Rev. Pharmacol. Toxicol. **39:** 399–430.

Collins, M. D., C. Eckhoff, R. Weiss, E. Resnick, H. Nau *et al.*, 2005 Differential teratogenesis of all-*trans*-retinoic acid in SWV and C57BL/6N mice administered at gestational day 9.5: emphasis on limb dysmorphology. Birth Defects Res. A Clin. Mol. Teratol. (in press).

Cordell, H. J., 2002 Epistasis: what it means, what it doesn't mean, and statistical methods to detect it in humans. Hum. Mol. Genet. **11:** 2463–2468.

Dai, W. S., J. M. LaBraico and R. S. Stern, 1992 Epidemiology of isotretinoin exposure during pregnancy. J. Am. Acad. Dermatol. **26:** 599–606.

Darvasi, A., 1998 Experimental strategies for the genetic dissection of complex traits in animal models. Nat. Genet. **18:** 19–24.

Daumer, K. M., A. C. Tufan and R. S. Tuan, 2004 Long-term in vitro analysis of limb cartilage development: involvement of Wnt signaling. J. Cell. Biochem. **93:** 526.

Deng, H. W., F. H. Xu, Q. Y. Huang, H. Shen, H. Deng *et al.*, 2002 A whole-genome linkage scan suggests several genomic regions potentially containing quantitative trait loci for osteoporosis. J. Clin. Endocrinol. Metab. **87:** 5151–5159.

Deng, H. W., H. Shen, F. H. Xu, H. Deng, T. Conway *et al.*, 2003 Several genomic regions potentially containing QTLs for bone size variation were identified in a whole-genome linkage scan. Am. J. Med. Genet. **119A:** 121–131.

Elmazar, M. M., U. Reichert, B. Shroot and H. Nau, 1996 Pattern of retinoid-induced teratogenic effects: possible relationship with relative selectivity for nuclear retinoid receptors RAR alpha, RAR beta, and RAR gamma. Teratology **53:** 158–167.

Fisher, R. A., 1918 The correlation between relatives on the supposition of Mendelian inheritance. Trans. R. Soc. Edinb. **52:** 399–433.

Geelen, J. A., 1979 Hypervitaminosis A induced teratogenesis. CRC Crit. Rev. Toxicol. **6:** 351–375.

Gong, Y., R. B. Slee, N. Fukai, G. Rawadi, S. Roman-Roman *et al.*, 2001 LDL receptor-related protein 5 (LRP5) affects bone accrual and eye development. Cell **107:** 513–523.

Hentges, K. E., M. Kyttala, M. J. Justice and L. Peltonen, 2004 Comparative physical maps of the human and mouse Meckel syndrome critical regions. Mamm. Genome **15:** 252–264.

Hovland, D. N., Jr., R. M. Cantor, G. S. Lee, A. F. Machado and M. D. Collins, 2000 Identification of a murine locus conveying susceptibility to cadmium-induced forelimb malformations. Genomics **63:** 193–201.

Jilka, R. L., R. S. Weinstein, K. Takahashi, A. M. Parfitt and S. C. Manolagas, 1996 Linkage of decreased bone mass with impaired osteoblastogenesis in a murine model of accelerated senescence. J. Clin. Invest. **97:** 1732–1740.

Jones, K. L., 1997 *Smith's Recognizable Patterns of Human Malformation.* W. B. Saunders, Philadelphia.

Kato, M., M. S. Patel, R. Levasseur, I. Lobov, B. H. Chang *et al.*, 2002 Cbfa1-independent decrease in osteoblast proliferation, osteopenia, and persistent embryonic eye vascularization in mice deficient in Lrp5, a Wnt coreceptor. J. Cell Biol. **157:** 303–314.

Lammer, E. J., D. T. Chen, R. M. Hoar, N. D. Agnish, P. J. Benke *et al.*, 1985 Retinoic acid embryopathy. N. Engl. J. Med. **313:** 837–841.

Lander, E., and L. Kruglyak, 1995 Genetic dissection of complex traits: guidelines for interpreting and reporting linkage results. Nat. Genet. **11:** 241–247.

Lander, E. S., P. Green, J. Abrahamson, A. Barlow, M. J. Daly *et al.*, 1987 MAPMAKER: an interactive computer package for constructing primary genetic linkage maps of experimental and natural populations. Genomics **1:** 174–181.

Lee, G. S., D. M. Kochhar and M. D. Collins, 2004 Retinoid-induced limb malformations. Curr. Pharm. Des. **10:** 2657–2699.

Majewski, F., H. Stoss, T. Goecke and H. Kemperdick, 1983 Are bowing of long tubular bones and preaxial polydactyly signs of the Meckel syndrome? Hum. Genet. **65:** 125–133.

Manly, K. F., R. H. Cudmore, Jr. and J. M. Meer, 2001 Map Manager QTX, cross-platform software for genetic mapping. Mamm. Genome **12:** 930–932.

Masinde, G. L., J. Wergedal, H. Davidson, S. Mohan, R. Li *et al.*, 2003 Quantitative trait loci for periosteal circumference (PC): identification of single loci and epistatic effects in F2 MRL/SJL mice. Bone **32:** 554–560.

Moore, K. J., and D. L. Nagle, 2000 Complex trait analysis in the mouse: the strengths, the limitations and the promise yet to come. Annu. Rev. Genet. **34:** 653–686.

Paavola, P., R. Salonen, J. Weissenbach and L. Peltonen, 1995 The locus for Meckel syndrome with multiple congenital anomalies maps to chromosome 17q21-q24. Nat. Genet. **11:** 213–215.

Paavola, P., K. Avela, N. Horelli-Kuitunen, M. Barlund, A. Kallioniemi *et al.*, 1999 High-resolution physical and genetic mapping of the critical region for Meckel syndrome and Mulibrey Nanism on chromosome 17q22-q23. Genome Res. **9:** 267–276.

Parr, B. A., and A. P. McMahon, 1995 Dorsalizing signal Wnt-7a required for normal polarity of D-V and A-P axes of mouse limb. Nature **374:** 350–353.

Pinson, K. I., J. Brennan, S. Monkley, B. J. Avery and W. C. Skarnes, 2000 An LDL-receptor-related protein mediates Wnt signalling in mice. Nature **407:** 535–538.

Podolin, P. L., P. Denny, C. J. Lord, N. J. Hill, J. A. Todd *et al.*, 1997 Congenic mapping of the insulin-dependent diabetes (Idd) gene, Idd10, localizes two genes mediating the Idd10 effect and eliminates the candidate Fcgr1. J. Immunol. **159:** 1835–1843.

Podolin, P. L., P. Denny, N. Armitage, C. J. Lord, N. J. Hill *et al.*, 1998 Localization of two insulin-dependent diabetes (Idd) genes to the Idd10 region on mouse chromosome 3. Mamm. Genome **9:** 283–286.

Shenefelt, R. E., 1972 Morphogenesis of malformations in hamsters caused by retinoic acid: relation to dose and stage at treatment. Teratology **5:** 103–118.

Shimizu, M., K. Higuchi, B. Bennett, C. Xia, T. Tsuboyama *et al.*, 1999 Identification of peak bone mass QTL in a spontaneously osteoporotic mouse strain. Mamm. Genome **10:** 81–87.

Sporn, M. B., A. B. Roberts and D. S. Goodman, 1994 *The Retinoids.* Raven Press, New York.

Sulik, K. K., and D. B. Dehart, 1988 Retinoic-acid-induced limb malformations resulting from apical ectodermal ridge cell death. Teratology **37:** 527–537.

Todd, J. A., T. J. Aitman, R. J. Cornall, S. Ghosh, J. R. Hall *et al.*, 1991 Genetic analysis of autoimmune type 1 diabetes mellitus in mice. Nature **351:** 542–547.

Villarroya, F., R. Iglesias and M. Giralt, 2004 Retinoids and retinoid receptors in the control of energy balance: novel pharmacological strategies in obesity and diabetes. Curr. Med. Chem. **11:** 795–805.

Wang, S., C. J. Basten and Z-B. Zeng, 2005 Windows QTL Cartographer 2.0. Department of Statistics, North Carolina State University, Raleigh, NC (http://statgen.ncsu.edu/qtlcart/WQTLCart.htm).

Wilson, J. G., 1973 *Environment and Birth Defects.* Academic Press, New York.

Xu, S., and W. R. Atchley, 1996 Mapping quantitative trait loci for complex binary diseases using line crosses. Genetics **143:** 1417–1424.

Yang, Y., L. Topol, H. Lee and J. Wu, 2003 Wnt5a and Wnt5b exhibit distinct activities in coordinating chondrocyte proliferation and differentiation. Development **130:** 1003–1015.

Zákány, J., C. Fromental-Ramain, X. Warot and D. Duboule, 1997 Regulation of number and size of digits by posterior Hox genes: a dose-dependent mechanism with potential evolutionary implications. Proc. Natl. Acad. Sci. USA **94:** 13695–13700.

Communicating editor: R. W. Doerge